Rozita Razavi,[1] Hamed S. Najafabadi,[2] Sarah Abdullah,[1] Simon Smukler,[1] Margot Arntfield,[1] and Derek van der Kooy[1]

Diabetes Enhances the Proliferation of Adult Pancreatic Multipotent Progenitor Cells and Biases Their Differentiation to More β-Cell Production

Diabetes 2015;64:1311–1323 | DOI: 10.2337/db14-0070

Endogenous pancreatic multipotent progenitors (PMPs) are ideal candidates for regenerative approaches to compensate for β-cell loss since their β-cell–producing capacities as well as strategic location would eliminate unnecessary invasive manipulations. However, little is known about the status and potentials of PMPs under diabetic conditions. Here we show that β-cell metabolic stress and hyperglycemia enhance the proliferation capacities of adult PMP cells and bias their production of progeny toward β-cells in mouse and human. These effects are dynamic and correlate with functional β-cell regeneration when conditions allow.

It is important to understand postnatal mechanisms of β-cell maintenance since β-cell dysfunction and loss are characteristics of both type 1 and type 2 diabetes (T1D and T2D) (1,2). Detection of β-cell regeneration under physiologic conditions such as pregnancy or diabetes predisposition is a relatively old concept (3,4), but the mechanisms involved, such as self-replication of pre-existing β-cells or participation of a stem-like cell population, are still the topic of ongoing debates. Nevertheless, the presence and contribution of adult pancreatic multipotent progenitor (PMP) populations in β-cell maintenance, particularly in injured pancreas, have been documented (5–7).

We reported a multipotent subpopulation of adult mouse and human islet cells that gives rise to cells of the endocrine, exocrine, as well as neuronal lineages (8). These PMPs are the developmental progeny of a $Pdx1^+$ cell population and express insulin in adult tissue (9). Indeed, these PMP cells resemble immature β-cells with low granularity and low to zero expression of β-cell–specific glucose transporter, Glut2 (8,9). These single $insulin^+Glut2^{low}$ cells can be expanded clonally in vitro to form sphere colonies that consist of hundreds to thousands of cells. Transplantation of adult mouse and human PMP colonies under the kidney capsule of diabetic mice was able to ameliorate hyperglycemia (9). Their ability to produce insulin may be the main reason that these cells were ignored in most lineage tracing studies as well as in studies that suggested β-cell replication as the main source of regeneration and where insulin was used as a designated marker for mature β-cells (10–12).

The presence of such a potent cell population in normal adult pancreas prompted us to address their status and function under diabetic conditions. Here we used mouse models of diabetes in order to study the dramatic changes in the PMP population and their responses to various mechanisms of β-cell loss and stress. Our findings in mouse systems were also validated in diabetic human samples.

RESEARCH DESIGN AND METHODS

Animals, Tissue, and Cell Preparations

All studies were approved by the Office of Research Ethics at the University of Toronto. Mice used in these studies

[1]Department of Molecular Genetics, University of Toronto, Toronto, Ontario, Canada

[2]Donnelly Centre for Cellular and Biomolecular Research, University of Toronto, Toronto, Ontario, Canada

Corresponding author: Rozita Razavi, rozy.razavi@gmail.com.

Received 14 January 2014 and accepted 4 November 2014.

This article contains Supplementary Data online at http://diabetes.diabetesjournals.org/lookup/suppl/doi:10.2337/db14-0070/-/DC1.

included MIP-GFP transgenic CD1/Tg(Ins1-EGFP/GH1) 14Hara; wild-type and InsII-RFP transgenic C57BL/6 (The Jackson Laboratory); nonobese resistant (NOR), NOD, and NOD.*Scid* (The Jackson Laboratory); as well as Ins-rtTA;TET-DTA mice (supplied by the laboratory of Dr. Yuval Dor, The Hebrew University of Jerusalem). Animals were anesthetized using sodium pentobarbital prior to terminal procedures. Collagenase type IX (Sigma-Aldrich) perfusion through bile duct was used in order to digest pancreatic tissues.

For nuclear BrdU incorporation experiments, mice were treated with BrdU in their drinking water (0.2 mg/mL) for specified durations. Paraformaldehyde-perfused frozen pancreas of each mouse was sectioned at five levels. Insulin$^+$ cells with nuclear BrdU labeling within all islets from each level (per mouse) were quantified.

PMP Sphere Assay

For the clonal sphere formation assay, the mouse islets were handpicked after ficoll gradient selection of digested pancreas tissue (8). Similarly, human islets were handpicked from islet-enriched fractions that were provided by Alberta Diabetes Center. Islets were dissociated to single cells by trypsin incubation followed by manual trituration with siliconized small-borehole glass pipettes. Viable cells were counted using Trypan blue exclusion and plated at 10,000 or 5,000 cells in a volume of 1 mL (clonal density) within each well of a 24-well plate (each well having a surface area of 2 cm^2). Cells were cultured in defined serum-free medium (SFM) (13) containing B27 (Gibco-BRL), 10 ng/mL FGF2 (Sigma-Aldrich), 2 μg/mL heparin (Sigma-Aldrich), and 20 ng/mL EGF (Sigma-Aldrich) for 14 days in uncoated 24-well plates (BD Falcon). Clonality of PMP spheres was tested previously by culturing single dissociated cells of the islets (one cell per well) (8). Mouse and human colonies were categorized based on their diameters. Resultant spheres were differentiated by transferring individual spheres to wells coated with Matrigel basement membrane matrix (15.1 mg/mL stock diluted 1:25 in SFM; BD) in SFM containing 1% FBS for 7–14 days. The size distributions and proportions of spheres are consistent within the same strain but vary among different mouse strains and between mice and humans. There is not a significant difference in the proportion of differentiated progenies among the different size spheres of the same experimental group. However, to maintain consistency, always similar size spheres (and usually the largest sizes) from compared groups were selected for differentiation assays. The following assumptions were applied to the interpretation of sphere formation data: *1*) number of PMP colonies (large and small together) = number of PMP cells within the primary tissue, *2*) increased number of total colonies = expanded number of PMP cells in primary tissue, *3*) larger single PMP colonies = single PMP cells with enhanced proliferation capacity, *4*) increased number of large PMP colonies = enhanced proliferation of PMP cells, and *5*) small single PMP colonies = single PMP cells with less proliferation capacity. Samples in the sphere formation and differentiation assays were blinded to the experimenters.

Diabetes Induction

Diabetes was induced either by streptozocin (STZ) (Sigma-Aldrich) injection to wild-type, MIP-GFP, and Ins-RFP C57BL/6 male mice (The Jackson Laboratory) or by administration of doxycycline (Dexon; Sigma-Aldrich) in drinking water of Ins-rtTA;TET-DTA transgenic mice (shared by Dr. Yuval Dor). Blood glucose levels were monitored using the OneTouch Ultra Blood Glucose Meter (LifeScan, Inc., Milpitas, CA).

STZ was dissolved freshly in citrate buffer prior to injection, and a single dose of 200 mg/kg was injected intraperitoneally in 4–6-week-old male mice using 27-gauge needles. Daily monitoring of the blood glucose started 4 days after the injection. Diabetic animals were killed for further in vitro experiments.

Doxycycline (Dexon) was administered in the drinking water (200 μg/mL doxycycline, 2% weight for volume sucrose) of Ins-rtTA;TET-DTA mice. The water mixture was changed every 4 days. Fasting and nonfasting blood glucose levels were monitored weekly. Doxycycline-treated diabetic mice were kept in the absence of doxycycline for 3–5 months or killed for immediate experiments.

Flow Cytometry

Pancreatic cells were isolated as described, and cells were sorted with an EPICS Elite Cell Sorter (Beckman Coulter) or a FACSAria System (BD Biosciences). Glut2 sorting was performed after immunostaining of live cells (from Ins-RFP or MIP-GFP mice) or fixed cells (from Ins-rtTA;TET-DTA mice) with a primary anti-Glut2 rabbit antibody (IgG) (1:400; Chemicon and Santa Cruz Biotechnology, Dallas, TX), followed by staining with an Alexa 488 or Alexa 647 goat anti-rabbit secondary antibody (Santa Cruz Biotechnology). Pancreatic cells from Ins-rtTA;TET-DTA were fixed and stained for insulin using a primary monoclonal mouse antibody (IgG) (1:500; Sigma-Aldrich) and an Alexa 488–conjugated goat antibody. All cells from transgenic mice were sorted into positive and negative cell fractions on the basis of propidium iodide and fluorescein isothiocyanate fluorescence.

Insulin$^+$ cells from MIP-RFP and MIP-GFP transgenic mice were sorted to low and high Glut-expressing fractions for RNA extraction and sequencing analysis.

Immunocytochemistry and Histology

Immunostaining was performed on differentiated sphere colonies or pancreas frozen sections (8 μm). Samples were fixed in 4% paraformaldehyde and blocked using normal goat serum (10:100 PBS; BD Biosciences) for 1 h. For BrdU staining, an acid hydrolysis procedure using HCL (2 N) at 37°C for 30 min was performed prior to the blocking step.

Incubation with primary antibodies was at 4°C overnight. The primary antibodies used included anti-insulin mouse monoclonal (IgG) (1:500; Sigma-Aldrich), anti-insulin guinea

pig antibody polyclonal (IgG) (1:100; Abcam), antiglucagon mouse antibody monoclonal (IgG) (1:500; Sigma-Aldrich), and anti-BrdU rat monoclonal (IgG) (1:200; Abcam). Samples were then washed and incubated with Alexa-conjugated goat secondary antibodies (1:400, BD Biosciences) at room temperature for 1 h. Cell nuclei were counterstained with the nuclear dye Hoechst 33258 and colored blue.

RNA Sequencing Procedure and Data Analysis

Sorted insulin$^+$Glut2^{high} and insulin$^+$Glut2^{low} cells from control and STZ-treated MIP-GFP transgenic mice were collected separately. Total RNA extraction was performed on each sample using Norgen Biotek total RNA extraction kit (Thorold, Ontario, Canada). Total random sequencing was done using Illumina HiSeq2500 sequencer with V1 reagent and HiSeq Ribo-Zero depletion RNA protocol. Two lanes were used for each sample. Reads were mapped to the GRCm38 assembly of the mouse genome (mm10), using TopHat2 (14), guided by gene annotations from Ensembl (15). Duplicate reads, which are often artifacts of PCR amplification during library preparation, were then removed using SAMtools (16), and gene differential expression between samples was quantified using Cuffdiff (17), based on Ensembl gene annotations and with fragment bias correction (18).

Up/downregulated pathways were identified using Wilcoxon rank-sum test based on the logarithm of fold change of expression between pairs of samples, using pathway annotations from KEGG (19) and REACTOME (20), and significant enrichments were identified at Benjamini-corrected false discovery rate <0.05. The leading-edge set of genes for significant pathways, i.e., genes with the highest up- or downregulation, were then identified as described previously (21).

Statistics

Statistical analysis was performed using Prism software (GraphPad Software, La Jolla, CA) or R analysis platform (http://www.r-project.org/). Data are expressed as means ± SEMs, unless specified otherwise. Statistical comparisons between two groups were performed with a Student *t* test where appropriate, or by ANOVAs with Bonferroni or Tukey posttests for comparisons between groups. For nonparametric comparisons, Mann Whitney *U* test or Kruskal-Wallis test followed by Dunn multiple comparison test was performed depending on the number of samples. Data were considered significant when $P < 0.05$.

RESULTS

PMP Cells Are Hyperactive Under Acute β-Cell Stress

β-Cell function can be affected by direct cytotoxic insults as well as indirect physiologic changes such as hyperglycemia due to insulin resistance, all of which lead to β-cell stress defined by secretory and/or proliferative hyperactivity (22–24). Investigating the direct consequences of β-cell stress on PMP cells is limited due to the lack of a definitive marker for these cells. However, our previous data showed the enrichment of the insulin$^+$Glut2^{low} fraction of islet cells for the PMP population. In order to establish a baseline status for PMP cell gene expression, we performed a transcriptome analysis on both insulin$^+$Glut2^{low} and insulin$^+$Glut2^{high} sorted fractions of mature MIP-GFP transgenic islets using RNA sequencing. Gene ontology and transcriptome analysis of both fractions showed a significant enrichment for regulation of β-cell development and β-cell gene expression pathways in the insulin$^+$Glut2^{low} cell population ($\log_2$ false discovery rate >4, $P < 0.05$) (Supplementary Table 1). Numerous genes that are essential for β-cell development were upregulated in the insulin$^+$Glut2^{low} cell fraction (Fig. 1*A*). Curiously, the insulin$^+$Glut2^{low} cell fraction contained more Glut2 RNA transcripts. However, low expression of *MGAT4A* could explain the discrepancy in Glut2 mRNA and Glut2 protein expression in PMPs containing insulin$^+$Glut2^{low} cells (Fig. 1*A*). *MGAT4A* encodes GNT-4A glycosyltransferase, a Golgi-resident enzyme that prevents Glut2 degradation via N-glycosylation and is essential for consequent localization of Glut2 in the plasma membrane (25,26).

We then used sterptozocin (STZ)-induced diabetes as an acute β-cell stress and disease model with specific loss of mature β-cells that express the STZ-transporting molecule Glut2 (27–29). STZ enters β-cells through the β-cell–specific Glut2 channel and destroys the cells by induction of oxidative stress, which consequently leads to diabetes (29). The scarcity or lack of Glut2 presence on PMPs (9) permitted the prediction that these cells would be spared after STZ treatment. Thus, STZ-induced diabetes is a particularly suitable model to specifically address the reaction of PMP cells to hyperglycemia and β-cell loss. Single diabetogenic doses (200 mg/kg) of STZ were injected in 6–8-week-old CJ57BL/6 or MIP-GFP transgenic male mice (30). On day 4 or 5 postinjection, the STZ-injected mice showed elevated fasting blood glucose levels (Fig. 1*B*). These mice also exhibited typical symptoms of diabetes, such as dehydration, discolored urine, and elevated nonfasting blood glucose (Supplementary Fig. 1*A*). Transcriptome analysis of sorted insulin$^+$Glut2^{high} and insulin$^+$Glut2^{low} cell fractions from both control and STZ-treated diabetic islets revealed significant upregulation of 88 genes associated with cell cycle and DNA elongation pathways ($P < 0.05$) in diabetic insulin$^+$Glut2^{low} cells (Fig. 1*C*, *D*, and *E* and Supplementary Fig. 1*B* and Supplementary Table 2). This finding suggested that the proliferation capacities of diabetic PMPs should be enhanced.

We next performed PMP clonal sphere assays on the STZ- and vehicle-injected mice. As it was described for neurosphere formation assay previously (13), in the clonal sphere assay, the numbers and sizes (diameters) of spheres reflect the starting number of the PMP cells in islet tissue and their proliferative capabilities, respectively. The total number of clonal PMP spheres was elevated significantly in all STZ-injected mice, and these PMP cells also gave rise to more proliferating precursors that produced significantly larger (>200 μm) size spheres (Fig. 1*F*).

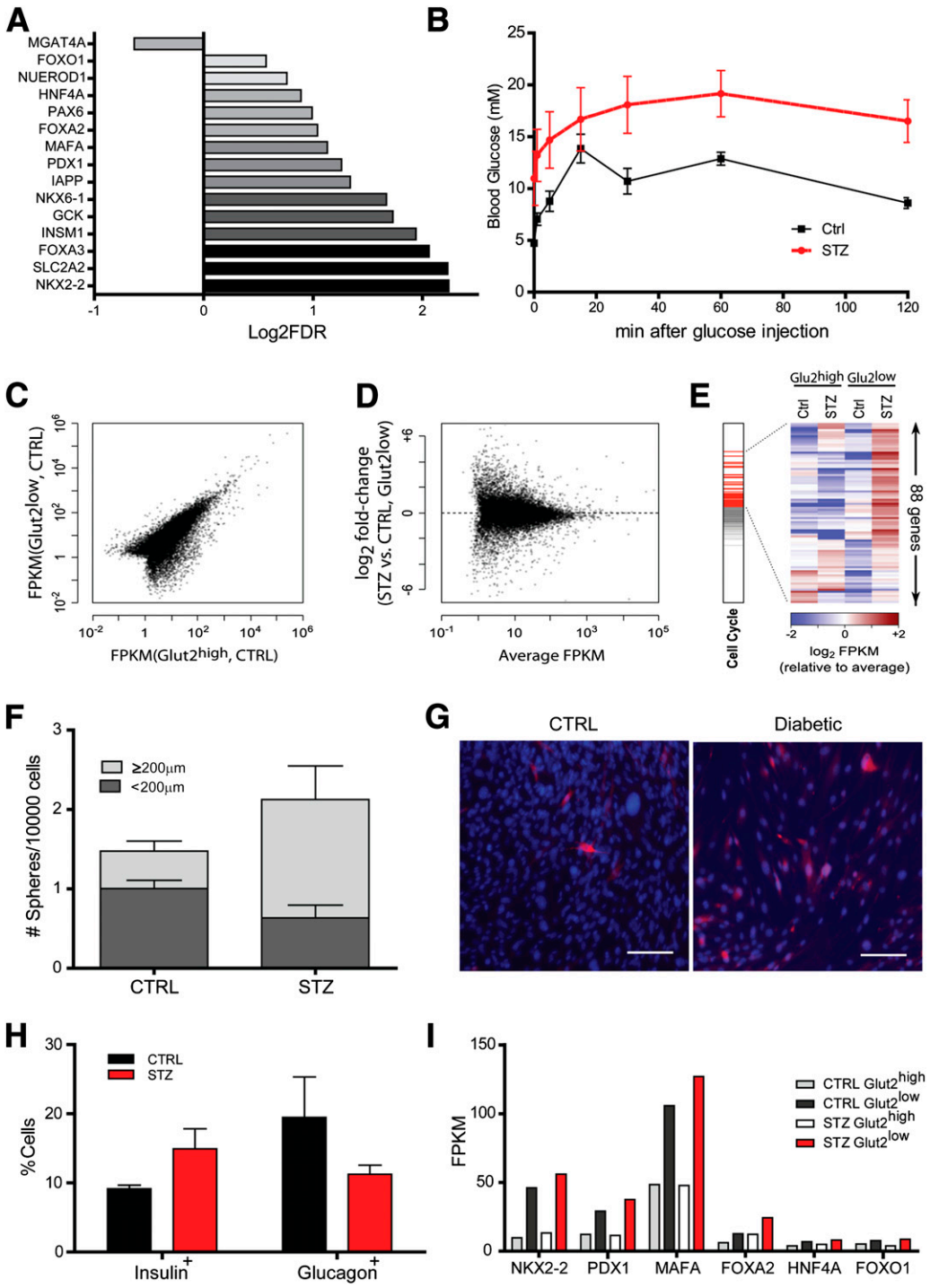

Figure 1—PMPs survive STZ cytotoxicity and produce larger colonies with a higher yield of insulin$^+$ progeny. *A*: Log_2 fold expression change (at $P < 0.05$) of genes involved in β-cell development pathway in insulin$^+$Glut2^{low} vs. insulin$^+$Glut2^{high} cells. *B*: Results of glucose tolerance tests performed on day 4 after STZ injection. Repeated-measures ANOVA comparing the two groups showed a significant effect of STZ/vehicle treatment ($F_{[1,8]} = 6.04$, $P = 0.045$, $n = 5$ mice/group). *C*: Scatterplot of measured FPKM (fragments per kilobase of transcript per million fragments) for insulin$^+$Glut2^{high} and insulin$^+$Glut2^{low} cells from control mice (CTRL). Only genes with FPKM >0 in both samples are shown. *D*: Differential gene expression in insulin$^+$Glut2^{low} cells of STZ-treated mice in comparison with control mice. Cell cycle genes, defined based on REACTOME annotations, are shown in *E*, with red bars corresponding to the "leading-edge" set of cell cycle genes. Cell cycle genes are significantly upregulated in insulin$^+$Glut2^{low} cells of STZ-treated mice relative to control mice (Wilcoxon rank sum test, $P < 0.002$). *E*: Expression of the leading-edge set of cell cycle genes across different samples. The majority of these genes are specifically expressed in Glut2^{low} cells of STZ-treated mice. *F*: Frequencies and diameter measures of PMP spheres from STZ-induced diabetic and control islets. Two-way ANOVA revealed a significant interaction of STZ-induced diabetes/vehicle treatment and the diameter of spheres ($F_{[1,11]} = 22.5$, $P = 0.006$), with a main effect of STZ/vehicle treatment ($F_{[1,8]} = 6.04$, $P = 0.045$). Bonferroni posttest showed a significant increase of large spheres in the STZ-treated group ($P < 0.05$, $n = 5$ mice/group). *G*: Immunofluorescent images of clonal differentiated PMP colonies derived from diabetic and control pancreata showing the insulin-expressing cells (red). Scale bar, 20 μm.

PMP clonal spheres were then transferred to serum-containing media for differentiation. Similar size clonal spheres from diabetic and nondiabetic groups were selected for comparing the progeny production by respective PMPs. Upon differentiation, diabetic spheres produced considerably higher numbers of insulin$^+$ cells compared with control (Fig. 1*G* and *H*), consistent with the elevated RNA levels of genes associated with β-cell development in diabetic insulin$^+$Glu2^{low} cells (Fig. 1*I*). The capacity of PMPs for producing non–β-cell pancreatic progeny was evaluated by quantifying glucagon$^+$ cells in differentiated colonies. Although the effect on the production of glucagon$^+$ progeny seems large, the bigger error bars prevented significance (Fig. 1*H*).

These data indicate that the PMP containing insulin$^+$Glut2^{low} cell population is resistant to STZ treatment in vivo. Moreover, the in vivo PMP population expands in STZ-induced diabetic islets and is more prone to insulin$^+$ cell production upon differentiation in vitro. Also, the consistency between the gene expression status of diabetic insulin$^+$Glut2^{low} cells and the status of diabetic PMP colonies supports the representation of PMP changes in vivo by sphere formation and differentiation assays in vitro.

Chronic β-Cell Stress Enhances the Proliferation Capacities of PMP Cells and Their β-Cell Production

In order to study the effects of ongoing chronic β-cell stress, we used NOD mice that spontaneously develop autoimmune diabetes with many similarities to T1D in humans (31,32). Various genetic abnormalities have been associated with NOD diabetes, some of which are β-cell dependent and autoimmune independent, such as β-cell stress. Previous studies have reported inherent abnormalities in NOD islet development with an augmented increase in islet size and β-cell mass around weaning time (4 weeks) followed by an accelerated turnover of β-cells and their consequent death (33). This chronic β-cell stress phenomenon is independent of the autoimmune attack since it is also seen in the NOD.*Scid* background that lacks immune system components (31,34,35). Thus, to dissect PMP properties under an inherent chronic β-cell stress, we also used NOD.*Scid* mice to avoid the complexities that are accompanied by autoimmune reactions.

To address the changes in the PMP population during postnatal islet development, adult pancreatic clonal sphere assays were performed on individual NOD.*Scid* mice at 4, 8, 12, and 15 weeks of age. The age-related kinetics in the NOD.*Scid* sphere assay data mimic the reported β-cell mass kinetics in vivo (33), with an increase in the number and size of the PMP colonies up until 8 weeks and a sharp decrease around 12 weeks (Fig. 2*A*). Comparing the numbers and sizes of NOD.*Scid* PMP colonies with its genetically closest "normal nondiabetic" strain, NOR mice that lack the β-cell stress (32), showed that the increased numbers and sizes of PMP spheres at 4–8 weeks (postnatal) is specific to NOD.*Scid* mice (Fig. 2*B*, left side). This situation reverses at 12–15 weeks of age when NOD.*Scid* islets seem to have less active progenitor cells than NOR (Fig. 2*B*, right side), possibly due to the proliferative exhaustion of the PMP cell pool during earlier stages of development.

In prediabetic NOD islets (4–6 weeks old), when the active autoimmune attack starts targeting insulin$^+$ cells, a decline in the total number of sphere-forming cells was observed when compared with nondiabetic NOR and C57BL/6 age-matched islets (Fig. 2*C* and *D*). At this stage, the observed decrease in NOD PMP population is absent in NOD.*Scid* and presumably reflects the loss of insulin$^+$ cells due to autoimmune attack.

Upon differentiation in serum-containing media, clonal NOD.*Scid* and NOD PMP spheres formed twice as many insulin$^+$ cells as NOR spheres. However, formation of glucagon$^+$ cells was not significantly different among the compared strains (Fig. 2*E*).

These findings demonstrate that in the NOD.*Scid* background, chronic β-cell stress is associated with an expansion of the PMP pool with enhanced ability to produce insulin$^+$ progeny. These capacities seem to be compromised in the presence of autoimmune attack, such as seen in NOD mice.

Enhanced Proliferation and Insulin$^+$ Cell Production Capacities of Diabetic Human PMP Cells

Similar to mouse, adult PMPs also have been identified in human pancreas (9). In order to verify the relevance of our findings in the context of human disease, we investigated the status of adult PMPs in the islet tissues obtained from diabetic and healthy human donors. Due to the scarcity of human diabetic donor tissue, we were able to obtain only three T1D samples over a period of 6 months. The islet-enriched fraction of each sample was received from the Alberta Diabetes Institute. Islets were handpicked and dissociated and were used for clonal sphere formation and differentiation assays as described previously (8).

All diabetic samples produced remarkably higher numbers of primary spheres compared with healthy

H: Frequencies of insulin$^+$ and glucagon$^+$ progeny produced by differentiated clonal PMP spheres from STZ-induced diabetic islets and controls. Two-way ANOVA indicated the significant interaction of diabetes and hormone$^+$ cell production ($F_{[1,28]} = 7.19$, $P = 0.0121$), with Bonferroni posttest showing increased number of insulin$^+$ cells in differentiated diabetic PMP colonies ($P < 0.05$, $n = 20$ spheres/group). Changes in glucagon$^+$ cell production were nonsignificant. *I*: FPKM of genes involved in β-cell development pathway are compared between insulin$^+$Glut2^{high} and insulin$^+$Glut2^{low} cells from diabetic and control islets. Values are means ± SEMs where error bars are shown. FDR, false discovery rate.

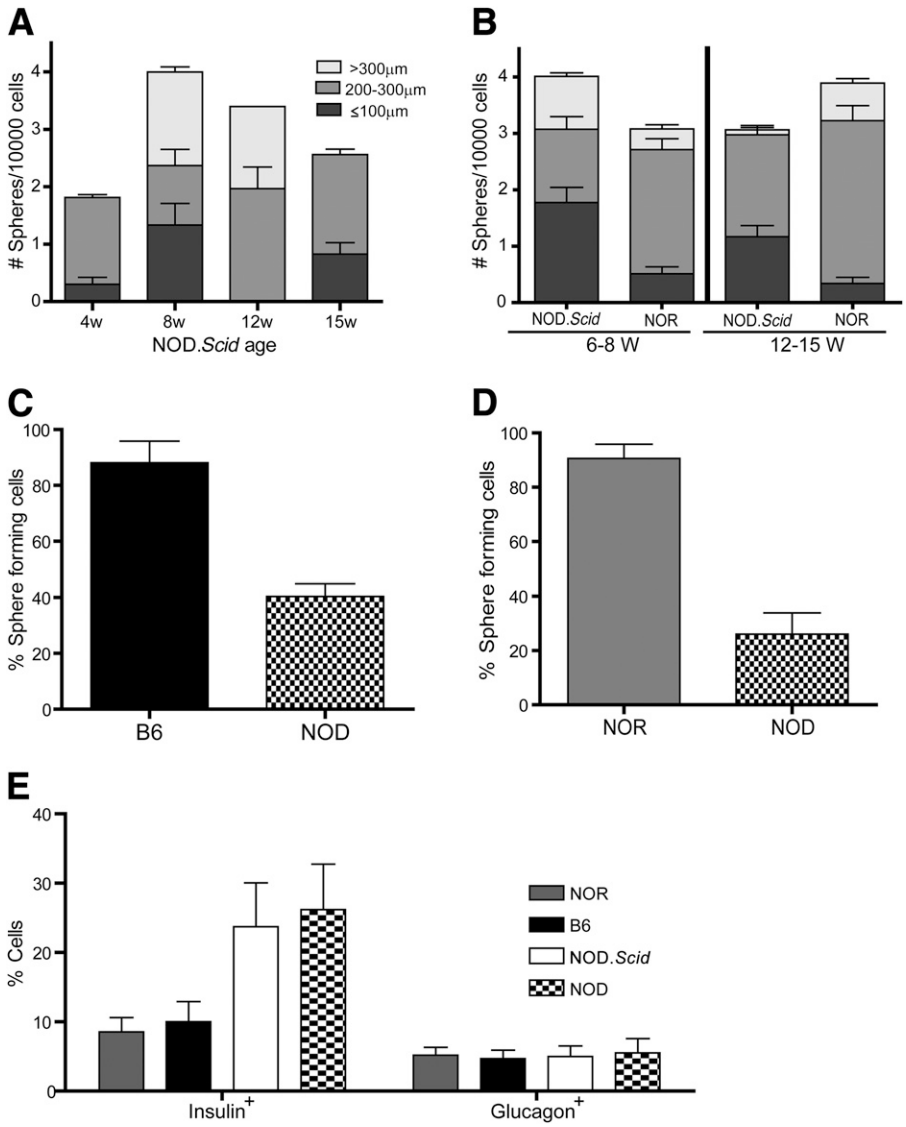

Figure 2—β-Cell stress in NOD mouse affects the pancreatic PMP cells. *A*: Frequencies and diameters of PMP sphere colonies derived from NOD.*Scid* islets at different ages. Two-way ANOVA revealed a significant interaction of age and sphere size ($F_{[6,368]} = 13.83$, $P < 0.0001$) with a main effect of age ($F_{[3,368]} = 12.41$, $P < 0.0001$). Bonferroni posttest comparing >300 μm and ≤100 μm size spheres showed a significant increase in the proportion of >300 μm spheres at 8 and 12 weeks of age ($P < 0.01$) when no small-size colonies (≤100 μm) were detectable, and a significant decrease in >300 μm spheres at 15 weeks of age ($P < 0.01$) when large spheres were no longer detectable ($n = 4$ mice/group). *B*: The frequencies and the diameters of PMP colonies from NOD.*Scid* and NOR pancreata at 6–8 and 12–15 weeks of age. Three-way ANOVA comparing age, strain, and sphere diameter showed a significant interaction of age and strain ($F_{[1,1]} = 10.005$, $P = 0.0017$), as well as strain and the diameter of spheres ($F_{[1,2]} = 34.3750$, $P < 0.0001$). The frequencies and diameter sizes of NOD.*Scid* PMP colonies at postweaning age of 6–8 weeks are greater than age-matched NOR spheres but decline to lower levels at 13–15 weeks ($n = 4$ mice/group). Frequencies of sphere-forming PMPs in 4–6-week-old female NOD mice and age-matched female mice from nondiabetic strains: C57BL/6 ($t = 5.527$, df = 10, $P < 0.0001$) (*C*) and NOR ($t = 6.847$, df = 10, $P < 0.0001$) (*D*); $n = 5$ or 6 mice/group. *E*: The frequencies of hormone-producing cells (insulin or glucagon) from differentiated PMP colonies. Size-matched spheres from NOD, NOD.*Scid*, B6, and NOR background were differentiated in serum-containing media and were separately stained for insulin or glucagon. Two-way ANOVA showed significant interaction of strain and hormone$^+$ cell production ($F_{[3,89]} = 23.32$, $P < 0.0001$), with Bonferroni posttest showing significant increases in insulin$^+$ cell production by NOD and NOD.*Scid* PMP colonies ($P < 0.05$, $n = 10$–15 spheres/group). No significant difference in glucagon$^+$ cell production was observed. The values are means ± SEMs. W, weeks.

controls (Fig. 3*A*). This trend was maintained after the primary spheres were passaged to form secondary and tertiary spheres (Supplementary Fig. 2*A* and *B*). The number of larger secondary spheres was expanded significantly in the diabetic samples (Supplementary Fig. 2*A*), confirming the enhanced proliferation capacity of T1D PMPs.

Upon differentiation in the presence of 1% serum for 2 weeks, the clonal spheres from human diabetic samples produced significantly higher percentages of insulin$^+$ and glucagon$^+$ cells compared with healthy controls (Fig. 3*B*, *C*, and *D*). Whereas the enhanced production of insulin$^+$ progeny was consistent in all individual diabetic samples

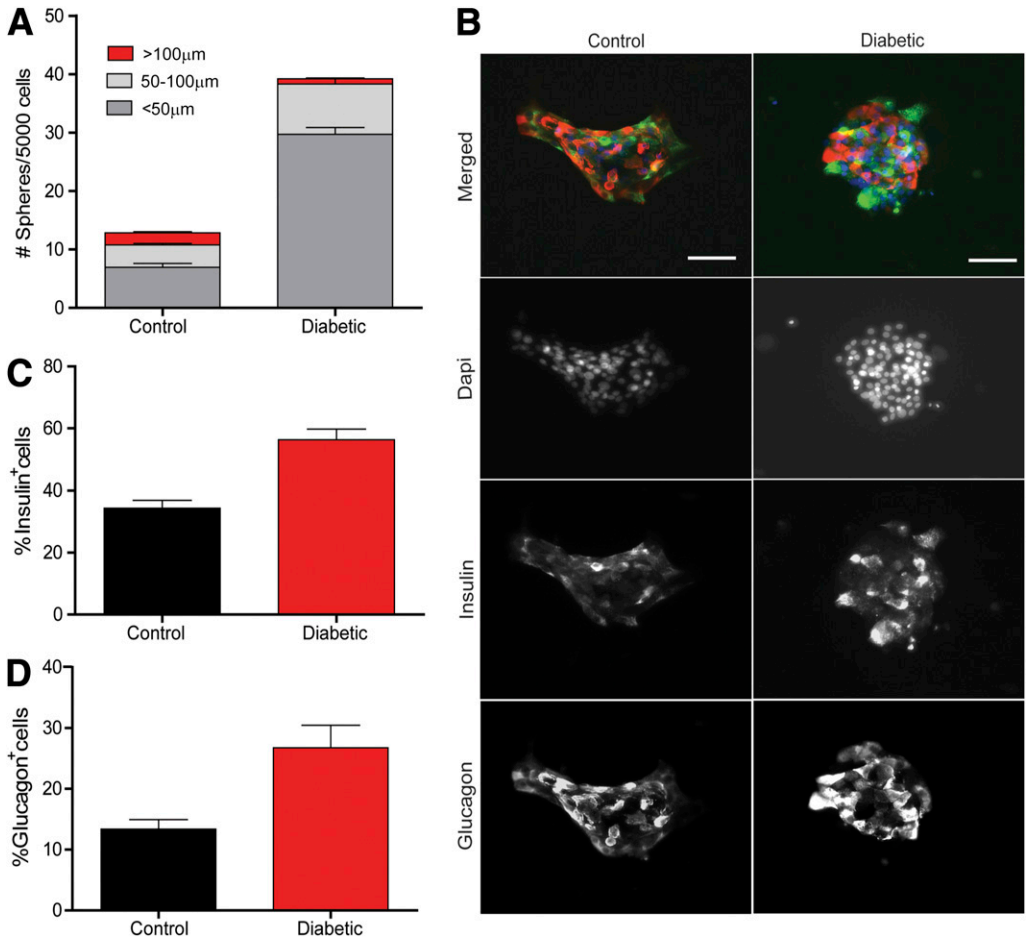

Figure 3—Behavior of human PMPs is altered under diabetic conditions. *A*: Frequencies and diameters of clonal PMP spheres produced from dissociated human islet cells. Islets were obtained from three healthy and three T1D donors and prepared for clonal sphere assays individually. Individual data from each group (control and diabetic) were combined. Two-way ANOVA revealed a significant interaction of diabetes and sphere diameter ($F_{[2,658]} = 114.97$, $P < 0.0001$), with a main effect of diabetes on total number of spheres ($F_{[1,658]} = 171.09$, $P < 0.0001$, n = 300–350 observed wells/group). *B*: Immunofluorescent images of differentiated single PMP colonies from diabetic and nondiabetic control human donors. *C* and *D*: Frequencies of insulin$^+$ (*C*) and glucagon$^+$ (*D*) cells produced from individual human PMP colonies. Single clonal spheres produced from three diabetic and two control human pancreatic islets were differentiated in serum-containing media for 2 weeks and were stained for insulin or glucagon expression. Data in both experiments were combined for each group (control and diabetic). Clonal spheres from diabetic samples produced greater numbers of insulin$^+$ cells (Mann-Whitney *U* test = 151, $P < 0.0001$) as well as greater numbers of glucagon$^+$ cells (Mann-Whitney *U* test = 278.5, $P < 0.012$). Number of analyzed spherical colonies in *B* and *C* is 20–40 per group. Values indicate mean ± SEMs. Scale bars, 50 μm.

(Supplementary Fig. 3*A*), the production of glucagon$^+$ cell progeny by diabetic spheres did not follow a steady pattern (Supplementary Fig. 3*B*).

Consistent with the data above from mouse diabetic models, these findings suggest that the adult human PMP population expands under diabetic conditions and possesses a larger capacity to produce β-cell–like cells.

PMP Status Reflects β-Cell Regeneration During Diabetic Recovery

To investigate the involvement of adult PMPs in diabetes-induced β-cell regeneration, we used a reversible diabetic mouse model. The double-transgenic Ins-rtTA;TET-DTA mice specifically express diphtheria toxin subunit A (DTA) in β-cells upon doxycycline administration, which leads to diabetes (36). These mice develop diabetes after DTA activation, and then a few weeks after the DTA expression has ended, they become euglycemic due to β-cell regeneration (36). The confounding factors of other models of diabetes, such as polygenetic background contributions, autoimmune destruction of newly formed β-cells, and the nonspecific toxicity or universal pancreas injury of chemically induced diabetes, have been minimized in these transgenic mice (36).

We used these mice as an established model of β-cell regeneration to investigate the status of PMPs throughout the diabetes and recovery processes. Doxycycline was administered through the drinking water to 6–8-week-old transgenic mice for 7–10 days. Mice that developed diabetes either were killed at the onset of hyperglycemia for PMP sphere assays or were maintained without further

doxycycline exposure, and their blood glucose levels were monitored weekly until euglycemia was achieved. The clonal pancreatic sphere assays were performed on these mice at weeks 8 and 14 after doxycycline treatment.

As previously reported, fasting and nonfasting blood glucose levels were elevated in doxycycline-treated Ins-rtTA;TET-DTA mice, and the glucose tolerance tests revealed their disturbed glucose homeostasis (Fig. 4*A*). The diabetic mice regained normoglycemia after 4–8 weeks postdoxycycline treatment, and their normal blood glucose level was maintained throughout the remainder of the experiment (Fig. 4*B*). At the onset of diabetes (10–14 days postdoxycycline treatment), the clonal sphere assay showed a significant decrease in the number of clonal PMP colonies in diabetic pancreata (Fig. 4*C*). The numbers of pancreatic sphere colonies reached control levels by the

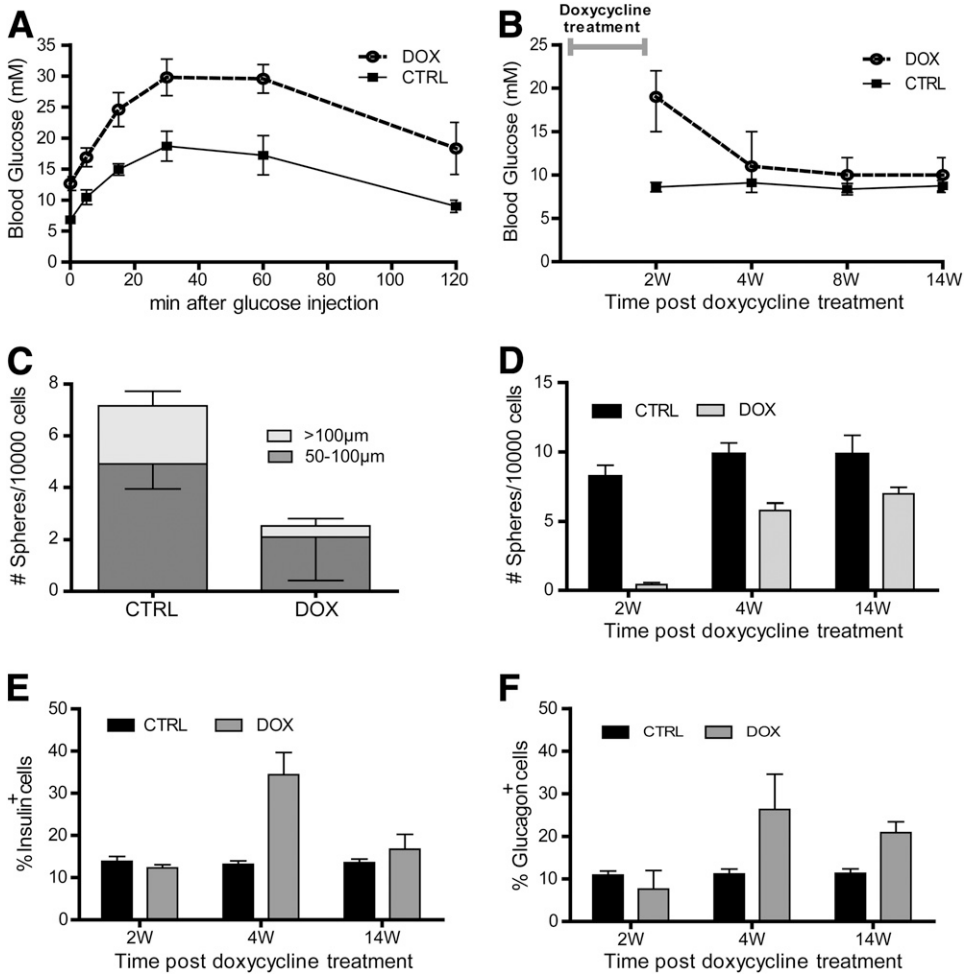

Figure 4—In vivo behavior of PMPs reflects the kinetics of postdiabetic β-cell regeneration. *A*: Results of glucose tolerance test performed on 4–6-week-old Ins-rtTA;TET-DTA transgenic mice after treatment ± doxycycline (DOX) in the drinking water for 2 weeks. Repeated-measures ANOVA comparing the two groups showed a main effect of doxycycline treatment ($F_{[1,8]}$ = 12.83, P = 0.0231, n = 5–10 mice/group). CTRL, control. *B*: Changes of blood glucose levels in diabetic Ins-rtTA;TET-DTA mice following termination of doxycycline treatment (n = 10 mice/groups). Repeated-measures ANOVA comparing the two groups indicated a significant interaction of blood glucose level and time ($F_{[3,24]}$ = 11.96, P < 0.0001), with Bonferroni multiple comparison test showing a significant blood glucose difference only at 2 weeks (P < 0.0001, n = 5 mice/group). *C*: Frequencies and diameters of clonal spheres derived from pancreatic islet cells of doxycycline-treated diabetic Ins-rtTA;TET-DTA mice vs. vehicle-treated controls. Two-way ANOVA indicated a main effect of doxycycline-induced diabetes/vehicle treatment ($F_{[1,91]}$ = 142.07, P < 0.0001), showing a significant reduction in the number of PMP colonies of diabetic mice (n = 5 pancreas/group). *D*: Frequencies of PMP colonies from doxycycline-treated diabetic Ins-rtTA;TET-DTA mice and their vehicle-treated controls at different time points after termination of doxycycline/vehicle treatment. Sphere assays were performed on recovering mice at 2, 4, and 14 weeks from the start of doxycycline/vehicle treatment. The first bar on the left (2 weeks) corresponds to the time of doxycycline/vehicle withdrawal. Two-way ANOVA revealed a significant interaction of doxycycline-induced diabetes/vehicle treatment and time ($F_{[2,118]}$ = 6.27, P = 0.0026, n = 5 mice/group). *E* and *F*: The frequencies of insulin$^+$ (*E*) and glucagon$^+$ (*F*) cell progeny developed by single PMP spheres derived from diabetic Ins-rtTA;TET-DTA pancreata compared with their corresponding controls throughout the recovery period. Two-way ANOVA showed a main effect of doxycycline-induced diabetes/vehicle treatment ($F_{insulin[1,29]}$ = 11.8, P = 0.0023, and $F_{glucagon[1,21]}$ = 4, P = 0.0389, n = 6–10 spheres/group), with Bonferroni posttest showing significant expansion of both progenies at week 4 (P < 0.01) that declined over time with insulin$^+$ cell production returning to control levels. Values are means ± SEMs, except for panel *C* where the values for the small-size spheres (60–100 μm) are indicated as means minus SEMs for clarity. W, weeks.

4th week after doxycycline treatment and close to the time of normoglycemic restoration (Fig. 4*D*). At the onset of diabetes, the diabetic clonal spheres produced comparable numbers of differentiated insulin$^+$ cells and glucagon$^+$ cells to controls (Fig. 4*E* and *F*, 2-week groups). However, the PMP colonies of recovering islets produced more than twice as many insulin$^+$ cells and glucagon$^+$ cells as differentiated control colonies (Fig. 4*E* and *F*, 4-week groups). The increased production of insulin$^+$ cells by diabetic colonies decreased back to control level after 6 more weeks (or 14 weeks postdoxycycline treatment) (Fig. 4*E* and *F*, 14-week groups).

These data document the dynamic changes of adult PMP cells throughout the β-cell restoration process, with increases in proliferation and the production of hormone$^+$ cell progeny, that later decline as the diabetic condition reverses and blood glucose levels normalize.

In Vivo Changes in PMP Population Under Diabetic Condition

The lack of definitive markers for adult PMPs is a major obstacle for investigating the normal physiologic or diabetes-induced changes at the cellular level in vivo. Nevertheless, this adult PMP population expresses insulin and minimal or undetectable levels of Glut2 (9), which could be used to probe the status of these cells in freshly isolated tissue. We measured the number of insulin$^+$Glut2^{low} cells in the pancreata of diabetic mice by flow cytometry in order to assess the in vivo changes in the PMP population.

InsII-RFP transgenic mice that express red fluorescent protein under the control of insulin promoter were rendered diabetic following injection of a single diabetogenic (200 mg/kg) dose of STZ, and their islets were dissected and dissociated as previously described (8,30). Dissociated live islet cells were stained for Glut2 expression (Fig. 5*A*). Analysis of FACS data revealed a significant increase of about twofold in the proportion of the insulin$^+$Glut2^{low} population within diabetic islets, along with a total decrease in the number of RFP$^+$ cells (presumably dying mature β-cells) (Fig. 5*B*). This finding is consistent with the diabetogenic effects of STZ, which destroy the mature Glut2-expressing β-cells and spare the Glut2^{low}-expressing PMP population.

In order to test the possible change in the PMP population throughout normoglycemia recovery, we used the transgenic Ins-rtTA;TET-DTA mouse model. Doxycycline was added to drinking water of Ins-rtTA;TET-DTA mice for 2 weeks, and blood glucose was measured to detect diabetic mice. In parallel, other Ins-rtTA;TET-DTA mice (rendered diabetic previously) were weaned off doxycycline for 1–2 weeks. The end point was the same for all experiments that had different starting points, in order to have consistent experimental conditions, and the treatment was blinded to the experimenter. The dissociated islet cells were fixed, permeabilized, and stained for insulin as well as Glut2 expression. FACS analyses revealed a significant decrease in the insulin$^+$Glut2^{low} population of doxycycline-treated diabetic islets immediately after doxycycline treatment (Fig. 5*C* and *D*, 2 week), which reflects the global loss of many insulin$^+$ cells due to DTA activation. However, the insulin$^+$Glut2^{low} cell population reached control levels 2 weeks postdoxycycline withdrawal (Fig. 5*D*, 4 week), which mirrors the activation of the PMP population observed in the sphere assay experiment.

In another experiment, we added BrdU to the drinking water of Ins-rtTA;TET-DTA mice either at the start of doxycycline treatment or at the 4th week postdoxycycline treatment. Mice that received BrdU at the beginning of doxycycline treatment were killed in week 4 posttreatment, and the other group was killed in week 14. Quantification of insulin$^+$BrdU$^+$ cells per islet showed a significant increase in the number of divided cells at 4 weeks, which was reduced after this time (Fig. 5*E*–*H*).

These findings show that changes in the activities of diabetic PMPs depend on the mechanism of β-cell loss or regeneration and that the in vivo changes match the changes seen in the in vitro sphere assay in these same cell populations. Moreover, the data suggest that the potential contribution of PMP cells to β-cell regeneration continues until the normoglycemia is achieved.

DISCUSSION

Previously, we detected a small insulin$^+$Glut2^{low} PMP cell population that contributes to endocrine, exocrine, and neuronal components of islet tissue under normal conditions (8,9). However, it was unclear whether or not islet insult prompts these cells to a more active state that would compensate for the β-cell loss. Since a definitive marker for these PMP cells has not been characterized, and because the sorted insulin$^+$Glut2^{low} fraction of islet cells is enriched for the colony-forming PMP cells, we applied their insulin$^+$Glut2^{low} expression characteristic to study their status during diabetes and recovery process. Collectively our data demonstrate that β-cell stress and hyperglycemia increase the numbers of PMPs in vivo, their proliferation capacity, and induce a bias toward production of more insulin$^+$ differentiated cell progeny by these cells.

To our knowledge, this is the first report that adult PMPs attempt to compensate (and successfully so under certain conditions) for β-cell loss in human and mouse pancreas. Several previous studies indicate that self-replication of preexisting β-cells is the main mechanism of β-cell regeneration elicited by β-cell loss. This mechanism essentially represents acceleration of an otherwise slow-paced self-replicating process that occurs under normal conditions (36–38). In contrast, acute insults such as pancreatectomy or ductal ligation provoke neogenesis as opposed to self-replication as the major mechanism of β-cell regeneration (7,39–41). In these studies, neogenesis was induced due to major physical or genetic manipulations of the tissue in order to detect β-cell regeneration (pancreatectomy, ductal ligation, and genetic manipulation) (7,29–33). The neogenesis was carried out by precursor-like

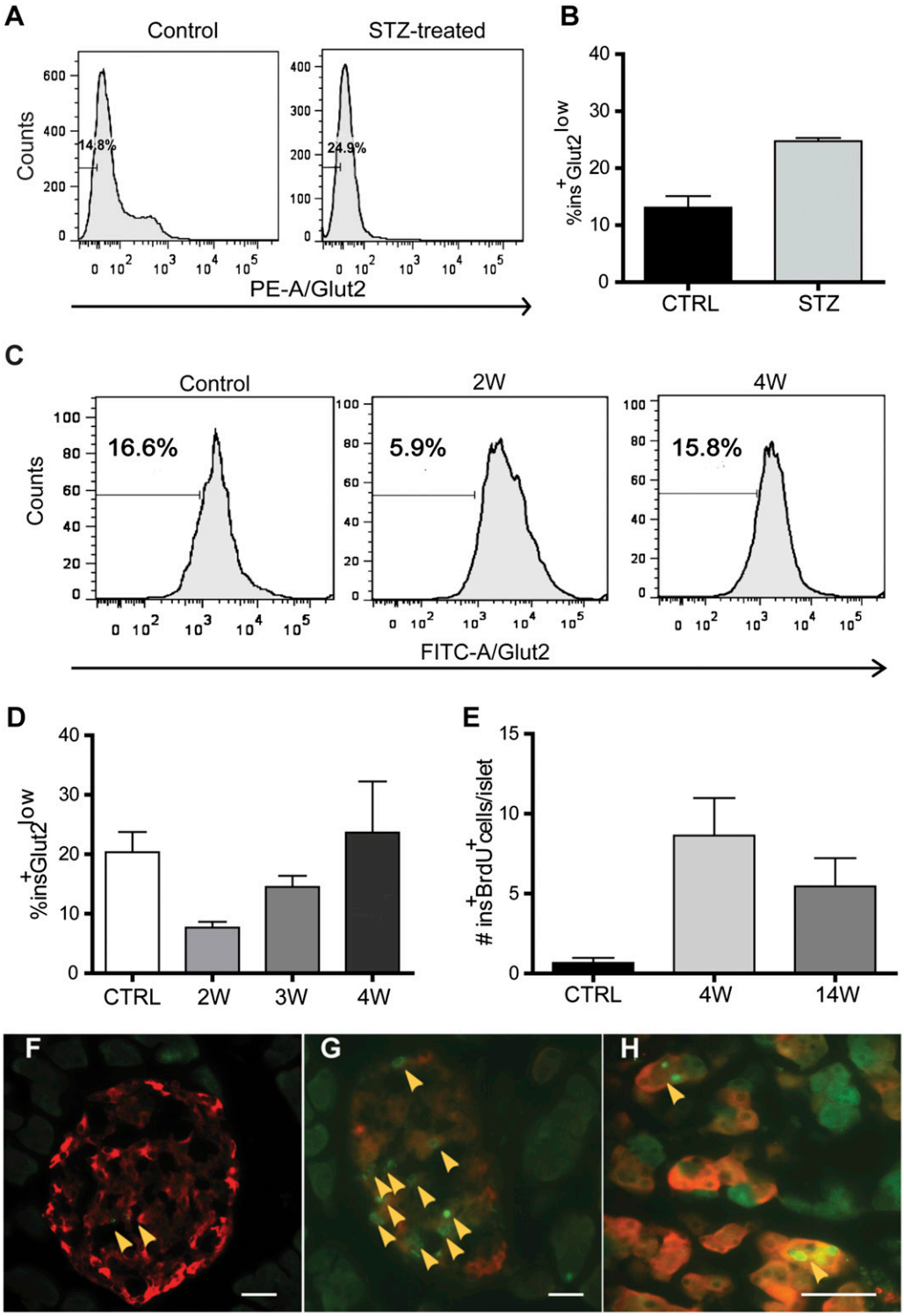

Figure 5—Status of PMP containing insulin$^+$Glut2^{low} cell population reflects the in vivo changes in β-cell (and β-cell regeneration) during diabetes and recovery process. *A*: FACS analysis of pancreatic islet cells from control and STZ-induced InsII-RFP diabetic mice for insulin$^+$Glut2^{low} cell populations. Low to zero expression of Glut2 was defined using live unstained RFP$^+$ population of islet cells. *B*: Comparison of Glut2^{low} cell percentage of insulin$^+$ cells from STZ-induced diabetic and control (CTRL) islets (t = 5.492, df = 7, n = 4 mice, 1–2 × 10^4 counts/sample, P = 0.0015). *C*: FACS analysis of insulin$^+$Glut2^{low} cell populations of doxycycline- and vehicle-treated Ins-rtTA;TET-DTA transgenic mice. Fixed and permeabilized islet cells were stained for both insulin and Glut2. Low to zero expression of Glut2 was defined using an insulin-expressing (fluorescein isothiocyanate$^+$ [FITC$^+$]) population of Ins-rtTA;TET-DTA islet cells in the absence of Glut2 staining. *D*: Percentages of insulin$^+$Glut2^{low} cell population from Ins-rtTA;TET-DTA diabetic pancreata compared with control after doxycycline withdrawal. 2W indicates the termination of doxycycline treatment. Analyzing the data using Kruskal-Wallis test as well as Dunn multiple comparison test showed significant reduction of insulin$^+$Glut2^{low} cells at 2 weeks (P = 0.0372, n = 3–6 mice/group). *E–H*: BrdU labeling of proliferating islet cells of Ins-rtTA;TET-DTA mice. BrdU was added (0.2 mg/mL) to drinking water of mice either

cells that either resided in the ductal epithelium or were spontaneously produced by *trans* differentiation or dedifferentiation of acinar or ductal cells (39,42,43). In another study, cytokine treatment of overtly diabetic mice induced *trans* differentiation of acinar cells to β-cell–like cells (44). Our findings suggest that preexisting progenitor-like cells can contribute to β-cell compensation elicited by naturally occurring β-cell stress such as that observed in NOD/NOD.*Scid* mice, as well as in human diabetic samples.

Moreover, the temporal changes in adult PMP and their differentiated progenies during the recovery from diabetes in Ins-rtTA;TET-DTA mice (Supplementary Fig. 4) provide evidence for the contribution of adult PMPs to functional β-cell recovery. A previous study on β-cell regeneration used these same transgenic mice and reported β-cell replication as the main mechanism for β-cell compensation (36). However, in that study, insulin was considered as a marker for only mature β-cells and not potential progenitors. Another study (45) used a similar transgenic line, but reported that near total loss of β-cells induced α-cell conversion to β-cells. Thorel et al. (45) used a pulse-chase strategy to label α-cells in a glucagon-rtTA-R26-YFP transgenic mouse line harboring doxycycline-inducible RIP-DTR transgene prior to induction of diabetes. Their tetracycline pulse labeled 90% of all α-cells with yellow fluorescent protein (YFP) expression, but only 65% of the regenerated β-cells were YFP labeled. No significant change in the α-cell mass and up to 44-fold increase in β-cell mass during recovery were reported (45). Although this evidence supported the potential conversion of some glucagon$^+$ cells to insulin$^+$ cells, no explanation was provided regarding the possible source(s) for the rest of the regenerated YFP$^-$ β-cells. Therefore, involvement of preexisting double hormone$^+$ (insulin$^+$glucagon$^+$) as well as glucagon$^-$YFP$^-$ cell populations that may contain PMPs cannot be excluded in this regeneration process. Total or near-total abrogation of α-cells, as described previously by the same investigators (46), prior to induction of diabetes and the consequent recovery would have differentiated the presence of non–α-cell origin of regenerated β-cells.

Unlike the increased production of differentiated insulin$^+$ progeny from PMPs in all of the diabetic models, we did not observe a consistent pattern for the production of differentiated glucagon$^+$ progeny. Nevertheless, single diabetic PMP colonies produced a smaller proportion of noninsulin$^+$ cells that contained glucagon$^+$ progeny than nondiabetic PMPs. This phenotype suggests the impact of diabetes and β-cell stress on PMPs to selectively act toward compensating for lost β-cells. Enhanced cell cycle pathway and upregulated β-cell development genes such as *PDX1*, *MAFA1*, and *NKX2.2* (47) in the diabetic insulin$^+$Glut2^{low} cell population support this conclusion (Fig. 1*I*). However, investigating the mechanisms by which diabetes elicits such effects is hampered by the lack of more specific in vivo markers for PMP cells.

Increased β-cell mass due to hyperglycemia has been associated with cell-autonomous molecular mechanisms that increase β-cell proliferation such as cell cycle regulators (cycline D family) (48,49), systemic factors such as hormones (insulin and prolactin) (4), and glucose (50). In a mouse model of insulin resistance, it was shown that betatrophin, a newly discovered molecule produced by hepatocytes, could increase β-cell proliferation and normalize blood glucose levels (51). These mechanisms could also underlie the activation process of cell cycle pathways as well as β-cell development pathways that we found to be enriched in PMP containing insulin$^+$Glut2^{low} cells under diabetic conditions. Nonetheless, the robust presence of hyperactive adult PMP cells with enhanced potential for β-cell production within the diabetic islets of mice and humans opens up new possibilities for regenerative applications in diabetes.

Current regenerative approaches for treating human diabetes has concentrated almost entirely on the production of new β-cells from human pluripotent stem cell systems (52–55). Moreover, most evidence for the presence of stem/progenitor cell–like populations in nondissociated adult human pancreatic tissue has been limited to detecting equivocal stem cell marker expression in various pancreatic cell types (53,55–57). Here for the first time, we report that β-cell stress/hyperglycemia stimulates an adult tissue progenitor cell population within human islets to proliferate and produce more insulin$^+$ progeny. Interestingly, PMPs from aged, nondiabetic human islets showed similar trends (Supplementary Fig. 4). Perhaps expansion of PMPs in these islets is associated with β-cell stress due to aging (58,59).

Our findings suggest that in T1D, efficient control of recurring autoimmune reactions to insulin$^+$ cells could facilitate β-cell restoration by PMPs. Examples such as partial recovery of NOD mice from diabetes after blocking the

throughout the doxycycline/vehicle treatment period (2 weeks) or in week 4 after the start of doxycycline treatment. Mice that received BrdU at the start of doxycycline treatment were killed at 4 weeks, and the other group was killed at 14 weeks. Pancreas sections were stained for insulin (red) and BrdU (green), and insulin$^+$BrdU$^+$ cells were counted in each islet. *E*: Number of insulin$^+$BrdU$^+$ cells per islets in doxycycline-treated mice after 4 and 14 weeks compared with vehicle-treated controls at 14 weeks. One-way ANOVA indicated a significant difference in the number of insulin$^+$BrdU$^+$ cells among experimental groups ($F_{[2,200]} = 6.742$, $P = 0.0041$), with Tukey multiple comparison test showing significant increases in insulin$^+$BrdU$^+$ cells in the doxycycline-treated group at 4 and 14 weeks ($P < 0.0001$, $n = 3$ mice/group, 15–30 islets/mouse). *F–H*: Representative micrographs for control and doxycycline-treated islets. Arrowheads indicate insulin$^+$BrdU$^+$ cells. *F*: The highest observed number of nuclear insulin$^+$BrdU$^+$ cells in a control islet. *G*: Nuclear BrdU labeling of insulin$^+$ cells in a recovering islet at 4 weeks. *H*: Nuclear BrdU$^+$ doublets showing the newly divided insulin$^+$ cells at 4 weeks. Values are means ± SEMs. Scale bar, 20 μm. W, weeks.

autoimmune reaction with anti-CD8 antibodies (60) support the efficiency of such approaches. A clear future goal is to promote the mechanisms that positively control this potent endogenous regeneration process within the context of β-cell loss and to minimize the opposing factors.

Acknowledgments. The authors thank Dr. Mike Wheeler and his laboratory members, Dr. Kacey Prentice, Dr. Emma Allister, and Dr. Alexandre Hardy (Department of Physiology, University of Toronto), for providing and preparing human pancreatic samples; Dr. Yuval Dor (Hebrew University of Jerusalem) for generously providing Ins-rtTA;TET-DTA transgenic mice; Dr. Allen Rosebrock (Department of Molecular Genetics, University of Toronto) and Dr. Timothy R. Hughes (Department of Molecular Genetics, University of Toronto) for providing advice on transcriptome analysis; Dr. Weijia Wang (The Institute of Biomaterials and Biomedical Engineering [IBBME], University of Toronto) for assistance with flow cytometry; Lillian Riad-Allen (University of Toronto) for advising on statistical analysis; and Brenda Coles (University of Toronto) for technical support.

Funding. This work was supported by JDRF (16-2006-465) and the Canadian Institutes of Health Research (MOP-123444). R.R. was supported by both Canadian Institutes of Health Research (MEF-95149) and McEwen fellowships (307212).

Duality of Interest. No potential conflicts of interest relevant to this article were reported.

Author Contributions. R.R. designed and performed experiments, analyzed data, and wrote the manuscript. H.S.N. analyzed RNA-sequencing data, prepared corresponding figures, and wrote materials and methods of the RNA-sequencing section. S.A. helped with diabetes monitoring and the sphere assay. S.S. provided data and necessary information for the manuscript revision. M.A. assisted with the sphere assay experiments. D.v.d.K. designed experiments, analyzed data, and wrote the manuscript. D.v.d.K. is the guarantor of this work and, as such, had full access to all the data in the study and takes responsibility for the integrity of the data and the accuracy of the data analysis.

Prior Presentation. Parts of this study were presented in abstract form at the 11th Annual Meeting of the International Society for Stem Cell Research, Boston, MA, 12–15 June 2013.

References

1. Tourrel C, Bailbe D, Lacorne M, Meile MJ, Kergoat M, Portha B. Persistent improvement of type 2 diabetes in the Goto-Kakizaki rat model by expansion of the beta-cell mass during the prediabetic period with glucagon-like peptide-1 or exendin-4. Diabetes 2002;51:1443–1452

2. Yan P, Cheah JS, Thai AC, Yeo PP. Current concepts of the pathogenesis and management of diabetic ketoacidosis (DKA). Ann Acad Med Singapore 1983; 12:596–605

3. Nielsen JH, Svensson C, Galsgaard ED, Møldrup A, Billestrup N. Beta cell proliferation and growth factors. J Mol Med (Berl) 1999;77:62–66

4. Kim H, Toyofuku Y, Lynn FC, et al. Serotonin regulates pancreatic beta cell mass during pregnancy. Nat Med 2010;16:804–808

5. Bonner-Weir S, Baxter LA, Schuppin GT, Smith FE. A second pathway for regeneration of adult exocrine and endocrine pancreas. A possible recapitulation of embryonic development. Diabetes 1993;42:1715–1720

6. Fernandes A, King LC, Guz Y, Stein R, Wright CV, Teitelman G. Differentiation of new insulin-producing cells is induced by injury in adult pancreatic islets. Endocrinology 1997;138:1750–1762

7. Xu X, D'Hoker J, Stangé G, et al. Beta cells can be generated from endogenous progenitors in injured adult mouse pancreas. Cell 2008;132:197–207

8. Seaberg RM, Smukler SR, Kieffer TJ, et al. Clonal identification of multipotent precursors from adult mouse pancreas that generate neural and pancreatic lineages. Nat Biotechnol 2004;22:1115–1124

9. Smukler SR, Arntfield ME, Razavi R, et al. The adult mouse and human pancreas contain rare multipotent stem cells that express insulin. Cell Stem Cell 2011;8:281–293

10. Dor Y, Brown J, Martinez OI, Melton DA. Adult pancreatic beta-cells are formed by self-duplication rather than stem-cell differentiation. Nature 2004;429: 41–46

11. Brennand K, Huangfu D, Melton D. All beta cells contribute equally to islet growth and maintenance. PLoS Biol 2007;5:e163

12. Xiao X, Chen Z, Shiota C, et al. No evidence for β cell neogenesis in murine adult pancreas. J Clin Invest 2013;123:2207–2217

13. Tropepe V, Sibilia M, Ciruna BG, Rossant J, Wagner EF, van der Kooy D. Distinct neural stem cells proliferate in response to EGF and FGF in the developing mouse telencephalon. Dev Biol 1999;208:166–188

14. Kim D, Pertea G, Trapnell C, Pimentel H, Kelley R, Salzberg SL. TopHat2: accurate alignment of transcriptomes in the presence of insertions, deletions and gene fusions. Genome Biol 2013;14:R36

15. Hubbard T, Barker D, Birney E, et al. The Ensembl genome database project. Nucleic Acids Res 2002;30:38–41

16. Li H, Handsaker B, Wysoker A, et al.; 1000 Genome Project Data Processing Subgroup. The Sequence Alignment/Map format and SAMtools. Bioinformatics 2009;25:2078–2079

17. Trapnell C, Williams BA, Pertea G, et al. Transcript assembly and quantification by RNA-Seq reveals unannotated transcripts and isoform switching during cell differentiation. Nat Biotechnol 2010;28:511–515

18. Roberts A, Trapnell C, Donaghey J, Rinn JL, Pachter L. Improving RNA-Seq expression estimates by correcting for fragment bias. Genome Biol 2011;12:R22

19. Kanehisa M, Goto S, Sato Y, Kawashima M, Furumichi M, Tanabe M. Data, information, knowledge and principle: back to metabolism in KEGG. Nucleic Acids Res 2014;42:D199–D205

20. Croft D, O'Kelly G, Wu G, et al. Reactome: a database of reactions, pathways and biological processes. Nucleic Acids Res 2011;39:D691–D697

21. Subramanian A, Tamayo P, Mootha VK, et al. Gene set enrichment analysis: a knowledge-based approach for interpreting genome-wide expression profiles. Proc Natl Acad Sci U S A 2005;102:15545–15550

22. Amrani A, Durant S, Throsby M, Coulaud J, Dardenne M, Homo-Delarche F. Glucose homeostasis in the nonobese diabetic mouse at the prediabetic stage. Endocrinology 1998;139:1115–1124

23. Fourlanos S, Narendran P, Byrnes GB, Colman PG, Harrison LC. Insulin resistance is a risk factor for progression to type 1 diabetes. Diabetologia 2004; 47:1661–1667

24. Bernard-Kargar C, Ktorza A. Endocrine pancreas plasticity under physiological and pathological conditions. Diabetes 2001;50(Suppl. 1):S30–S35

25. Luni C, Marth JD, Doyle FJ 3rd. Computational modeling of glucose transport in pancreatic β-cells identifies metabolic thresholds and therapeutic targets in diabetes. PLoS ONE 2012;7:e53130

26. Ohtsubo K, Chen MZ, Olefsky JM, Marth JD. Pathway to diabetes through attenuation of pancreatic beta cell glycosylation and glucose transport. Nat Med 2011;17:1067–1075

27. Matkovics B, Kotorman M, Varga IS, Hai DQ, Varga C. Oxidative stress in experimental diabetes induced by streptozotocin. Acta Physiol Hung 1997-1998; 85:29–38

28. Wang Z, Gleichmann H. Glucose transporter 2 expression: prevention of streptozotocin-induced reduction in beta-cells with 5-thio-D-glucose. Exp Clin Endocrinol Diabetes 1995;103(Suppl. 2):83–97

29. Schnedl WJ, Ferber S, Johnson JH, Newgard CB. STZ transport and cytotoxicity. Specific enhancement in GLUT2-expressing cells. Diabetes 1994;43: 1326–1333

30. Hayashi K, Kojima R, Ito M. Strain differences in the diabetogenic activity of streptozotocin in mice. Biol Pharm Bull 2006;29:1110–1119

31. Razavi R, Chan Y, Afifiyan FN, et al. TRPV1+ sensory neurons control beta cell stress and islet inflammation in autoimmune diabetes. Cell 2006;127:1123–1135

32. Leiter EH. The genetics of diabetes susceptibility in mice. FASEB J 1989;3: 2231–2241

33. Leiter EH. The NOD mouse: a model for insulin-dependent diabetes mellitus. Curr Protoc Immunol 2001;Chapter 15:Unit 15.9

34. Rosmalen JG, Homo-Delarche F, Durant S, Kap M, Leenen PJ, Drexhage HA. Islet abnormalities associated with an early influx of dendritic cells and macrophages in NOD and NODscid mice. Lab Invest 2000;80:769–777
35. Rosmalen JG, Pigmans MJ, Kersseboom R, Drexhage HA, Leenen PJ, Homo-Delarche F. (2001). Sex steroids influence pancreatic islet hypertrophy and subsequent autoimmune infiltration in nonobese diabetic (NOD) and NODscid mice. Lab Invest 2001;81:231–239.
36. Nir T, Melton DA, Dor Y. Recovery from diabetes in mice by beta cell regeneration. J Clin Invest 2007;117:2553–2561
37. Bouwens L, Rooman I. Regulation of pancreatic beta-cell mass. Physiol Rev 2005;85:1255–1270
38. Tavana O, Zhu C. Too many breaks (brakes): pancreatic β-cell senescence leads to diabetes. Cell Cycle 2011;10:2471–2484
39. Bonner-Weir S, Inada A, Yatoh S, et al. Transdifferentiation of pancreatic ductal cells to endocrine beta-cells. Biochem Soc Trans 2008;36:353–356
40. Rosenberg L. Induction of islet cell neogenesis in the adult pancreas: the partial duct obstruction model. Microsc Res Tech 1998;43:337–346
41. Hayashi KY, Tamaki H, Handa K, Takahashi T, Kakita A, Yamashina S. Differentiation and proliferation of endocrine cells in the regenerating rat pancreas after 90% pancreatectomy. Arch Histol Cytol 2003;66:163–174
42. Rosenberg L. In vivo cell transformation: neogenesis of beta cells from pancreatic ductal cells. Cell Transplant 1995;4:371–383
43. Lipsett M, Finegood DT. Beta-cell neogenesis during prolonged hyperglycemia in rats. Diabetes 2002;51:1834–1841
44. Baeyens L, Lemper M, Leuckx G, et al. Transient cytokine treatment induces acinar cell reprogramming and regenerates functional beta cell mass in diabetic mice. Nat Biotechnol 2014;32:76–83
45. Thorel F, Népote V, Avril I, et al. Conversion of adult pancreatic alpha-cells to beta-cells after extreme beta-cell loss. Nature 2010;464:1149–1154
46. Thorel F, Damond N, Chera S, et al. Normal glucagon signaling and β-cell function after near-total α-cell ablation in adult mice. Diabetes 2011;60:2872–2882
47. Schwitzgebel VM, Scheel DW, Conners JR, et al. Expression of neurogenin3 reveals an islet cell precursor population in the pancreas. Development 2000; 127:3533–3542
48. Cozar-Castellano I, Takane KK, Bottino R, Balamurugan AN, Stewart AF. Induction of beta-cell proliferation and retinoblastoma protein phosphorylation in rat and human islets using adenovirus-mediated transfer of cyclin-dependent kinase-4 and cyclin D1. Diabetes 2004;53:149–159
49. Kushner JA. Beta-cell growth: an unusual paradigm of organogenesis that is cyclin D2/Cdk4 dependent. Cell Cycle 2006;5:234–237
50. Alonso LC, Yokoe T, Zhang P, et al. Glucose infusion in mice: a new model to induce beta-cell replication. Diabetes 2007;56:1792–1801
51. Yi P, Park JS, Melton DA. Betatrophin: a hormone that controls pancreatic β cell proliferation. Cell 2013;153:747–758
52. Montanucci P, Pennoni I, Pescara T, et al. The functional performance of microencapsulated human pancreatic islet-derived precursor cells. Biomaterials 2011;32:9254–9262
53. White MG, Al-Turaifi HR, Holliman GN, Aldibbiat A, Mahmoud A, Shaw JA. Pluripotency-associated stem cell marker expression in proliferative cell cultures derived from adult human pancreas. J Endocrinol 2011;211:169–176
54. Chandra V, Swetha G, Muthyala S, et al. Islet-like cell aggregates generated from human adipose tissue derived stem cells ameliorate experimental diabetes in mice. PLoS ONE 2011;6:e20615
55. Carlotti F, Zaldumbide A, Loomans CJ, et al. Isolated human islets contain a distinct population of mesenchymal stem cells. Islets 2010;2:164–173
56. Hanley NA, Hanley KP, Miettinen PJ, Otonkoski T. Weighing up beta-cell mass in mice and humans: self-renewal, progenitors or stem cells? Mol Cell Endocrinol 2008;288:79–85
57. Hald J, Galbo T, Rescan C, et al. Pancreatic islet and progenitor cell surface markers with cell sorting potential. Diabetologia 2012;55:154–165
58. Singh H, Farouk M, Bose BB, Singh P. Novel genes underlying beta cell survival in metabolic stress. Bioinformation 2013;9:37–41
59. Kaufman RJ. Beta-cell failure, stress, and type 2 diabetes. N Engl J Med 2011;365:1931–1933
60. Pechhold K, Koczwara K, Zhu X, et al. Blood glucose levels regulate pancreatic beta-cell proliferation during experimentally-induced and spontaneous autoimmune diabetes in mice. PLoS ONE 2009;4:e4827